Biochemical and Biophysical Research Communications 546 (2021) 145–149

Contents lists available at ScienceDirect

Biochemical and Biophysical Research Communications

journal homepage: www.elsevier.com/locate/ybbrc

Detection of bacterial colonization by the spectral changes of surface-enhanced Raman reporters

Maksim V. Gorbachevskii*, Sofia V. Filatova, Alla V. Filimonova, Dmitry S. Kopitsyn, Andrei A. Panchenko, Vladimir A. Vinokurov, Andrei A. Novikov

Gubkin University, Moscow, 119991, Russian Federation

ARTICLE INFO

Article history:
Received 11 January 2021
Accepted 28 January 2021
Available online 11 February 2021

Keywords:
SERS
Au nanoparticles
Biosensor
S. aureus
P. aeruginosa

ABSTRACT

In times of widespread multiple antibiotic resistance, the bacterial colonization of crucial medical surfaces should be detected as fast as possible. In this work, we present the non-destructive SERS method for the detection of bacterial colonization. SERS is an excellent tool for the monitoring of suitable substances in low concentrations. The SERS substrate was prepared by the aggregation of citrate-stabilized gold nanoparticles and the adsorption of the reporters (crystal violet, thiamine, and adenine). We have tested the substrate for the detection of clinically relevant *S. aureus* and *P. aeruginosa* bacteria. The SERS spectra before and after the substrate incubation revealed the degradation of the reporter by the growing bacteria. The growth of *P. aeruginosa* was detected using the substrates with preadsorbed crystal violet or adenine. The suitable reporter for the detection of *S. aureus* remains to be discovered. The selection of the reporters resistant to exposure but easily degraded by bacteria will open the way for the *in situ* monitoring of bacterial colonization, thus complementing the arsenal of methods in the battle against hospital infections.

© 2021 Elsevier Inc. All rights reserved.

1. Introduction

Bacterial colonization of various surfaces poses a grave threat in the hospital environment, especially when the medical devices are colonized by the bacteria with multiple antibiotic resistance [1–3]. Traditional diagnostic methods include bacterial growth and analysis using specific laboratory equipment such as culture methods or polymerase chain reaction assay (PCR). These methods are quite useful, but usually require prior information about the pathogen's possible nature, are time-consuming and expensive, and thus have limited applicability [4–7].

Microbiological diagnostics capabilities have increased significantly over the past decades. The modern express diagnostic methods register electrical conductivity or electrical capacity [8], heat flow [9], pressure drop [10], acoustic signal [11]. Most biosensors are designed to detect changes in the chemical composition of a growing population of bacteria.

Among different approaches for microbial analysis, spectral methods constitute a particular area of expertise. Optical biosensors are label-free and provide direct detection of bacteria or biofilms along with characteristic spectral profiles. Raman spectroscopy is a potentially powerful method for identifying and characterizing microorganisms [12,13]. The low-intensity Raman signal of bacteria can be amplified using the SERS approach [14–16]. A highly selective and sensitive SERS method enables the detection of bacteria, the differentiation of bacteria at the species or intraspecies level, and the investigation of specific chemical compositions of bacteria or biofilms [17–22].

The bacterial SERS spectra are often hard to interpret, overwhelmed with fluorescence, and have low intensity. SERS substrates could be modified with specific antibodies or aptamers to increase the sensitivity and selectivity of the sensor [23–25]. However, this approach significantly complicates the sensor production and raises its cost.

The detection of bacterial metabolites (e.g., pyocyanin of *Pseudomonas aeruginosa*) [27,28] or biomarkers (e.g., dipicolinic acid of *Bacillus anthracis*) [29] by SERS or SERRS is particularly promising.

In this paper, we show for the first time to our knowledge the indirect detection of the bacteria by the decrease of the SERS spectral signatures of the preadsorbed reporters. SERS substrates were prepared from citrate-stabilized gold nanoparticles. The SERS reporters (crystal violet, thiamine, and adenine) were adsorbed

* Corresponding author. 65 Leninsky Prospekt, Moscow, 119991, Russia.
E-mail address: slemwen@yandex.ru (M.V. Gorbachevskii).

https://doi.org/10.1016/j.bbrc.2021.01.099
0006-291X/© 2021 Elsevier Inc. All rights reserved.

onto the substrate, and their SERS spectra were registered before and after the incubation with bacteria.

2. Experimental section

2.1. Materials

Tetrachloroauric acid ($HAuCl_4 \cdot 3H2O$, 99.9%), sodium citrate dihydrate (99%), sodium bromide (≥99.5%), adenine hydrochloride hydrate (≥99%), thiamine hydrochloride (≥99%) were purchased from Sigma-Aldrich (St. Louis, MO, USA). Sodium hydroxide (99%), crystal violet, nitric acid (65%), hydrochloric acid (>35%) were acquired from Chimmed (Moscow, Russia). All chemicals were used as received without further purification. Deionized water with a resistivity of no less than 18 MΩ×cm (Simplicity UV, Millipore, USA) was used to prepare all aqueous solutions. Glassware was cleaned before use by soaking in freshly prepared *aqua regia* and rinsing with deionized water.

2.2. Synthesis of Au-seeds

For the synthesis of Au-seeds (~14 nm), 6 mL of deionized water, 71 mL of 25 mM HAuCl4 solution, and 88 mL of 60 mM sodium citrate solution were placed in a 10 mL polypropylene tube. The tube was sealed, and the solution was stirred and incubated at 90 °C for 15 min in the circulating water bath. As a result, a pink suspension of seed particles was formed. The seed suspension was gradually cooled to 15 °C in the water bath.

2.3. Seeded growth of AuNPs

The gold nanoparticles were synthesized according to a modified procedure from Bastus et al. [30]. Immediately after the synthesis of the Au-seeds, 40 mL of 25 mM $HAuCl_4$ solution and 40 mL of 60 mM sodium citrate solution were sequentially injected to the tube cooled to 15 °C. Then, the closed tube was placed in the water bath heated to 90 °C. After 30 min, the resulting dispersion was gradually cooled to 15 °C. These procedures were repeated three times. Then, 2 mL of the dispersion was taken from the tube, and 1.5 mL of deionized water was added. Starting from the third generation of gold particles, 40 mL of 25 mM $HAuCl_4$ solution, 40 mL of 60 mM sodium citrate solution, and a 60 mL portion of 25 mM NaOH solution were injected in each step. The synthesis was continued until the 18th generation of particles was collected [31].

2.4. Characterization of nanoparticles

For TEM analysis, 5 μL of nanoparticle dispersion was dropped on a formvar TEM grid (Ted Pella, Redding, CA, USA) and dried at room temperature. TEM micrographs were obtained using a JEM-2100 electron microscope (JEOL, Japan) at an accelerating voltage of 200 kV.

2.5. Preparation of SERS substrate plates

The schematic diagram of the experiment is shown in Fig. S1. Stainless steel plates (AISI 304 steel; 10 × 10 mm) were sonicated in acetone, then in ethanol, and were wrapped in aluminum foil. After that, SERS-active spots were cast by applying 2 μL of gold nanoparticles and 2 μL of reporter solution (or water). After that, the nanoparticles were aggregated by adding 2 μL 0.5 M of NaBr solution. Each plate contained four SERS spots. The analytes were deionized water (control), 1 μM crystal violet, 100 μM adenine, and 100 μM thiamine, four plates for each analyte. The experiments were triplicated; thus, we used 48 spots per analyte overall.

2.6. SERS measurements before and after the microbiological experiments

The SERS spectra were registered using a microscope (through a ×20 lens) equipped with the 785-nm BWS415 Raman spectrometer (BWTEK, Germany). The spectral resolution was 1.61–2.25 cm^{-1} over the 2000–400 cm^{-1} range. The laser power density was 2600 mW/mm^2. The acquisition time was 6 s. The SERS spectra were registered two hours after the analyte addition before the microbiological experiment. After the microbiological experiment, the plates were rinsed with water three times. For each SERS spot, seven spectra were registered from randomly selected points in the central area.

SERS spectra were processed automatically using Matlab subroutines [32]. Briefly, spectra were imported from the spectrometer-generated source data files; the fluorescence background was subtracted via a polynomial-fitting method [33]; the high-frequency noise was filtered, and the peak lists were extracted and exported to Excel files for visualization and interpretation. Peaks were compared by a maximum peak height in the selected range. The comparison was expressed as (mean ± sample standard deviation) of the peak height ratios. The selected ranges were 885–930 cm^{-1} for crystal violet, 740–774 cm^{-1} for thiamine, and 706–778 cm^{-1} for adenine.

2.7. Microbiological experiment with S. aureus and P. aeruginosa bacteria

The clinical isolates of *Staphylococcus aureus* (Mar 2013–119) and *Pseudomonas aeruginosa* (RES-2352) were used in the experiment. The cultures were grown on solid LB nutrient media for 24 h at 37 °C. A cell suspension with 0.5 McFarland standard density was prepared from the grown cultures.

The experiment design is presented in Table 1. The SERS plate, the cell suspension (20 μL), and Muller-Hinton broth (2.5 mL) were placed in the wells of the 12-well culture plate and incubated for 24 h in the dark. Saline solution and culture medium were used in the control wells.

2.8. SERS substrate quality control after the experiment

The adenine solution aliquot (3 μL, 100 μM) was applied after the SERS measurements on the sample A/*P. aeruginosa*. The drop was air-dried at 25 °C, and the plate was washed in water and dried again. The SERS analysis was repeated. For each SERS spot, seven spectra were taken from randomly selected points in the central area.

2.9. Statistical analysis

The statistical significance of the observed changes in the samples was assessed by the one-way analysis of variance (ANOVA) with the Matlab subroutines.

3. Results and discussion

The SERS substrate was prepared using gold nanoparticles on stainless steel plates. In contrast to silver nanoparticles, gold nanoparticles do not emit metal ions noticeably, and therefore are more stable. Thus, one could expect better stability of SERS substrates prepared from gold nanoparticles. In addition, gold nanoparticles themselves do not have a bactericidal effect [34]. We used 18th-generation gold nanoparticles (AuNPs) with a 41.2 ± 3.5 nm diameter and the extinction maximum at 532.1 nm (Fig. S2).

All forty-eight SERS substrate plates were examined by SERS

Table 1
Microbiological experiment design.

	Medium/Bacterial culture			
	Control (saline solution)	Control (bacteria medium)	*Staphylococcus aureus* (*S. aureus*)	*Pseudomonas aeruginosa*
(O) Control (without reporter)	O/Saline	O/Medium	O/*S. aureus*	O/*P. aeruginosa*
(CV) Crystal Violet 10^{-6} M	CV/Saline	CV/Medium	CV/*S. aureus*	CV/*P. aeruginosa*
(B1) Thiamine 10^{-4} M	B1/Saline	B1/Medium	B1/*S. aureus*	B1/*P. aeruginosa*
(A) Adenine 10^{-4} M	A/Saline	A/Medium	A/*S. aureus*	A/*P. aeruginosa*

spectroscopy before and after the microbiological experiment (Fig. 1).

The experiments were conducted according to the scheme presented in Table 1. The processed SERS spectra were compared before and after the microbiological experiment. The control samples (O) without reporter had no significant changes after the experiment. The samples of saline with microbes (O/*S. aureus* and O/*P. aeruginosa*) did not demonstrate the bacterial SERS spectra, probably due to the washing that removed the bacterial cells.

The crystal violet can be oxidized by a variety of bacteria but is also a biocide that reduces the possibility of its conversion by microorganisms [35,36]. After incubation with microbes, we estimated the spectra's changes by the ratio of the selected peak heights. Peak at 915 cm^{-1} related to bending ($CC_{center}C$) was selected for CV [37] for ease of analysis and spectral data processing (Fig. 1a). The value of $H_{915after}/H_{915before}$ for CV/Saline and CV/Medium control samples was 0.49 ± 0.08 and 0.56 ± 0.10, respectively (Fig. 1d). In the case of CV/Saline and CV/Medium samples, the decrease in intensity is explained by substrate erosion because of washing and incubation. The peak height decreased comparably in the CV/Saline and CV/Medium samples, although one could expect the larger decrease in the CV/Medium due to the competitive adsorption of the broth components (e.g., casein hydrolyzate).

In the samples with microbes, the $H_{915after}/H_{915before}$ values were 0.61 ± 0.15 for CV/*S. aureus* and 0.32 ± 0.16 for CV/*P. aeruginosa*. This difference suggests that *S. aureus* bacteria do not affect the CV dye, whereas *P. aeruginosa* decolorizes the dye significantly (Fig. S3). Bacteria can destroy dyes during growth [38,39], thereby decreasing their spectral intensity. It should be noted that *P. aeruginosa* strains actively decolorize textile dye effluent [40].

Curiously enough, thiamine spectral intensity increased in the several replications after the incubation in saline (Fig. 1e). For the B1/Saline sample, the $H_{756after}/H_{756before}$ value was 1.11 ± 0.51. The

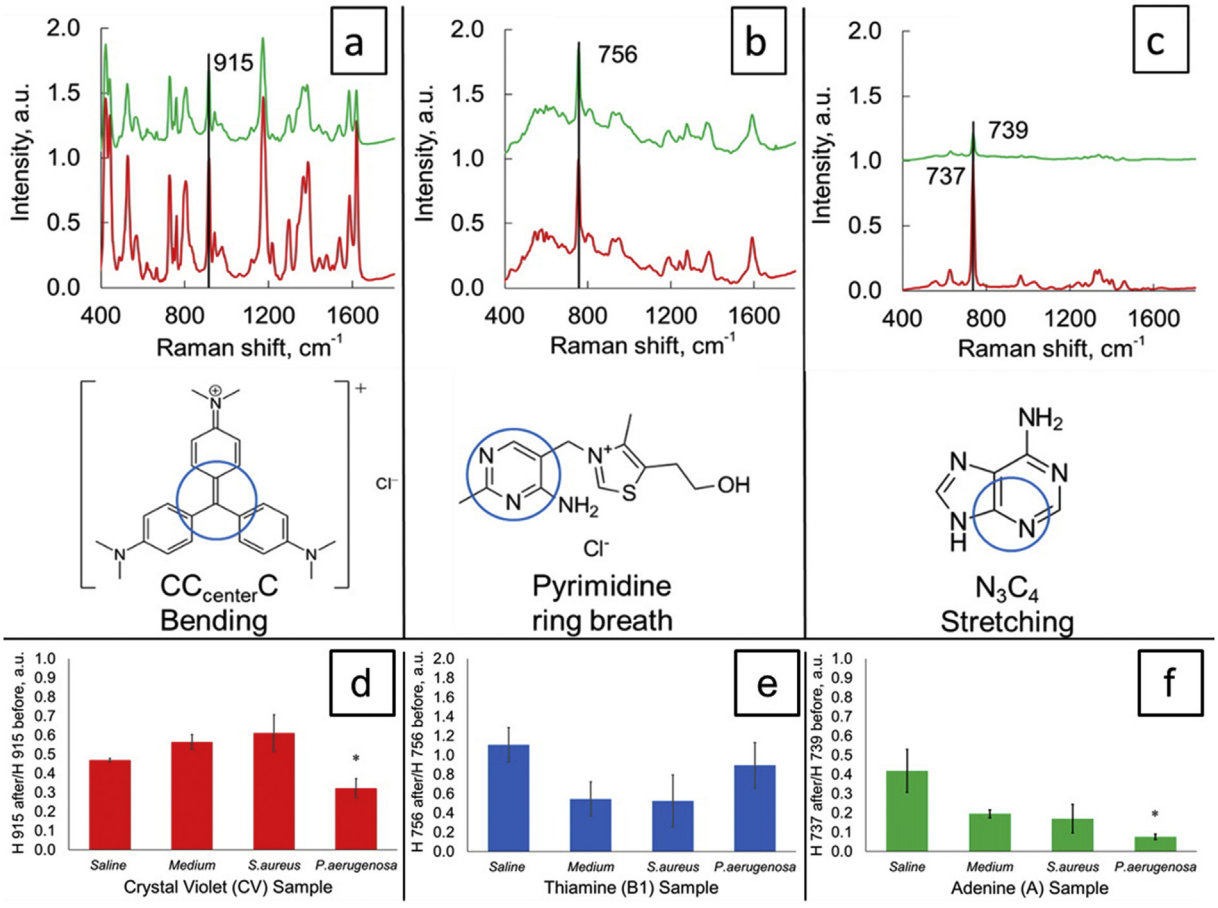

Fig. 1. SERS spectra of «Medium » samples before (red) and after (green) the microbiological experiment and structural formulae of compounds indicating vibrations of the studied peaks: crystal violet (a); thiamine (b); adenine (c). Selected peak ratios after/before the incubation. Crystal Violet $H_{915after}/H_{915before}$ (d); thiamine $H_{756after}/H_{756before}$ (e); adenine $H_{737after}/H_{739before}$ (f). The error bars show standard deviation. Asterisk (*) denotes significantly different from the Medium ($P < 0.05$). (For interpretation of the references to color in this figure legend, the reader is referred to the Web version of this article.)

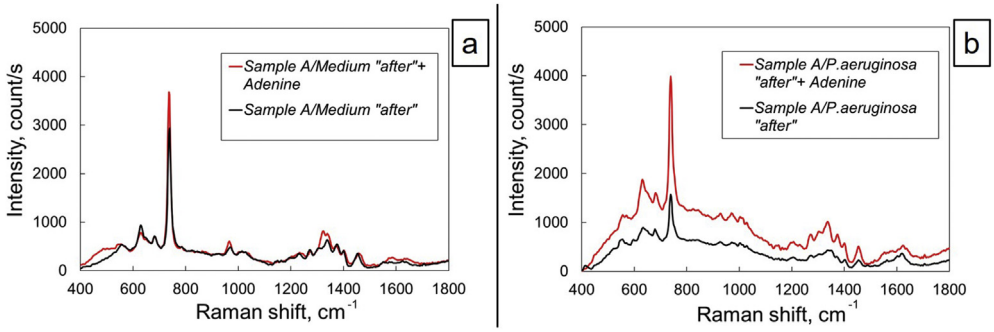

Fig. 2. Testing of SERS activity of the substrate after interaction with *P. aeruginosa*: the sample A/Medium immediately after incubation (black); the same sample with added 3 μL of 10^{-4} M adenine solution (red) (a); the sample A/*P. aeruginosa* immediately after incubation (black); the same sample with added 3 μL of 10^{-4} M adenine solution (red) (b). (For interpretation of the references to color in this figure legend, the reader is referred to the Web version of this article.)

protracted adsorption of thiamine may explain the increase in the spectral intensity and rather large standard deviation onto the hot spots of the SERS substrate. Previously, it was shown that rhodamine 6G requires about 30 min for complete adsorption on the surface of nanoparticles, while CV requires at least 1.5 h [31]. Another possible explanation is the thiamine conformation change due to the pH shift during the incubation. It is known that the intensity of the 755 cm^{-1} thiamine peak (Fig. 1b) is highly dependent on pH [41]. The initial pH of SERS substrate spots is around 4.5 (slightly acidic due to the citric acid/sodium citrate present at the nanoparticles' surface). The pH might increase to 6.5 during the incubation with saline, because we observed a 1590 cm^{-1} peak characteristic of unprotonated thiamine molecules.

For the B1/Medium, B1/*S. aureus*, and B1/*P. aeruginosa* samples, the $H_{756after}/H_{756before}$ values were 0.55 ± 0.25, 0.53 ± 0.33, and 0.89 ± 0.37, respectively (Fig. 1e). We can assume that *S. aureus* and *P. aeruginosa* do not metabolize the adsorbed thiamine because the spectral intensity does not significantly decrease when compared with the medium control (Fig. S4).

The adenine is easily metabolized by microorganisms [42]. We used the ratio of 737 cm^{-1} peak height before and 739 cm^{-1} peak height after the incubation to measure adenine spectral change ($H_{737after}/H_{739before}$). This peak corresponds to the adenosine ring's valent vibrations and is the most intense in the SERS adenine spectrum at the 785-nm excitation (Fig. 1c). The slight bathochromic shift of this peak is probably due to the pH change during the incubation. For the A/Saline and A/Medium samples, $H_{737after}/H_{739before}$ values were 0.42 ± 0.15 and 0.20 ± 0.04, respectively (Fig. 1f). This difference suggests that adenine gradually desorbs or decomposes in the deionized water; furthermore, adenine can be displaced from the gold nanoparticles by the culture medium components.

The peak height ratios differ for A/*S. aureus* and A/*P. aeruginosa* samples in the same manner as for CV samples. The $H_{737after}/H_{739before}$ value for A/*S. aureus* was 0.17 ± 0.07, which is close to the A/Medium value and suggests the inability of *S. aureus* to decompose the adsorbed adenine during the incubation. For *P. aeruginosa*, the $H_{737after}/H_{739before}$ value is 0.08 ± 0.03, which is significantly lower than the A/Medium and A/*S. aureus* values (Fig. S5). This decrease may be explained by the adenine decomposition or SERS substrate destruction by the bacteria. To rule out the latter possibility, we applied the extra amount of adenine to SERS spots that were incubated with culture medium with or without *P. aeruginosa*. We observed the significant increase in the adenine spectral intensity in the A/*P. aeruginosa* but not in the A/Medium sample. One can assume that adenine is displaced from the SERS-active hot spots by the culture medium components, and the addition of adenine after the incubation alter the spectral intensity only modestly (1.35 times) because the hot spots are not available (Fig. 2a). In contrast, in the A/*P. aeruginosa* sample, bacteria metabolize the adenine and the culture medium components, and the addition of adenine increases the spectral intensity 2.75 times because adenine adsorbs onto the vacated hot spots (Fig. 2b).

Thus, we can conclude that gram-positive *S. aureus* bacteria do not decompose crystal violet, adenine, and thiamine as monitored by SERS spectra. In contrast, gram-negative *P. aeruginosa* activity can be monitored by SERS spectra of crystal violet and adenine, but not thiamine. Therefore, even when the direct registration of bacterial spectra is impractical, the bacterial colonization of the surfaces can be detected using the coatings containing preformed SERS hot spots impregnated with suitable SERS reporter prone to the bacterial metabolic activity.

4. Conclusions

A new approach for the indirect detection of microorganisms by the SERS spectroscopy was demonstrated. The colonization of the aluminum substrate by *Pseudomonas aeruginosa* led to the degradation of crystal violet and adenine as evidenced by changes in their SERS spectra. The 915 cm^{-1} peak height of crystal violet decreased three times after the incubation in the medium inoculated with bacteria; and the 737 cm^{-1} peak of adenine shifted to the 739 cm^{-1}, and its height decreased to 8% of its original value. The demonstrated approach is a powerful technique that can be generalized for the express detection of the bacterial colonization by the selection of the appropriate SERS reporters. The desired SERS reporters (dyes or nitrogenous bases' derivatives) should strongly adsorb onto the gold nanoparticles surface, and be prone to the rapid degradation by the bacteria of interest.

Acknowledgments

The reported study was funded by the Ministry of Education and Science of the Russian Federation (Grant No. 14.Z50.31.0035). Maksim V. Gorbachevskii is grateful to the Russian Foundation for Basic Research (project number 19-38-90212) for financial support of PhD student's research.

Appendix A. Supplementary data

Supplementary data to this article can be found online at https://doi.org/10.1016/j.bbrc.2021.01.099.

Declaration of competing interest

The authors declare that they have no known competing financial interests or personal relationships that could have appeared to influence the work reported in this paper.

References

[1] A.G. Tkachenko, Stress responses of bacterial cells as mechanism of development of antibiotic tolerance (review), Appl. Biochem. Microbiol. 54 (2018) 108–127, https://doi.org/10.1134/S0003683818020114.

[2] B. Pelaz, C. Alexiou, R.A. Alvarez-Puebla, F. Alves, A.M. Andrews, S. Ashraf, L.P. Balogh, L. Ballerini, A. Bestetti, C. Brendel, S. Bosi, M. Carril, W.C.W. Chan, C. Chen, X. Chen, X. Chen, Z. Cheng, D. Cui, J. Du, C. Dullin, A. Escudero, N. Feliu, M. Gao, M. George, Y. Gogotsi, A. Grünweller, Z. Gu, N.J. Halas, N. Hampp, R.K. Hartmann, M.C. Hersam, P. Hunziker, J. Jian, X. Jiang, P. Jungebluth, P. Kadhiresan, K. Kataoka, A. Khademhosseini, J. Kopeček, N.A. Kotov, H.F. Krug, D.S. Lee, C.M. Lehr, K.W. Leong, X.J. Liang, M.L. Lim, L.M. Liz-Marzán, X. Ma, P. Macchiarini, H. Meng, H. Möhwald, P. Mulvaney, A.E. Nel, S. Nie, P. Nordlander, T. Okano, J. Oliveira, T.H. Park, R.M. Penner, M. Prato, V. Puntes, V.M. Rotello, A. Samarakoon, R.E. Schaak, Y. Shen, S. Sjöqvist, A.G. Skirtach, M.G. Soliman, M.M. Stevens, H.W. Sung, B.Z. Tang, R. Tietze, B.N. Udugama, J. Scott VanEpps, T. Weil, P.S. Weiss, I. Willner, Y. Wu, L. Yang, Z. Yue, Q. Zhang, Q. Zhang, X.E. Zhang, Y. Zhao, X. Zhou, W.J. Parak, Diverse applications of nanomedicine, ACS Nano 11 (2017) 2313–2381, https://doi.org/10.1021/acsnano.6b06040.

[3] K. Kalishwaralal, S. BarathManiKanth, S.R.K. Pandian, V. Deepak, S. Gurunathan, Silver nanoparticles impede the biofilm formation by Pseudomonas aeruginosa and Staphylococcus epidermidis, Colloids Surf. B Biointerfaces 79 (2010) 340–344, https://doi.org/10.1016/j.colsurfb.2010.04.014.

[4] N.M. Steele, J.H. Williamson, R. Thresher, R.A. Laven, J.E. Hillerton, Evaluating a commercial PCR assay against bacterial culture for diagnosing Streptococcus uberis and Staphylococcus aureus throughout lactation, J. Dairy Sci. 100 (2017) 3816–3824, https://doi.org/10.3168/jds.2016-11752.

[5] M.E. Collins, E.B. Popowitch, M.B. Miller, Evaluation of a novel multiplex PCR panel compared to quantitative bacterial culture for diagnosis of lower respiratory tract infections, J. Clin. Microbiol. 58 (2020), https://doi.org/10.1128/JCM.02013-19.

[6] J. Kuypers, K.R. Jerome, Applications of digital PCR for clinical microbiology, J. Clin. Microbiol. 55 (2017) 1621–1628, https://doi.org/10.1128/JCM.00211-17.

[7] S.J. Salipante, K.R. Jerome, Digital PCR—an emerging technology with broad applications in microbiology, Clin. Chem. 66 (2020) 117–123, https://doi.org/10.1373/clinchem.2019.304048.

[8] T. Kim, J. Kang, J.H. Lee, J. Yoon, Influence of attached bacteria and biofilm on double-layer capacitance during biofilm monitoring by electrochemical impedance spectroscopy, Water Res. 45 (2011) 4615–4622, https://doi.org/10.1016/j.watres.2011.06.010.

[9] J. Lerchner, A. Wolf, F. Buchholz, F. Mertens, T.R. Neu, H. Harms, T. Maskow, Miniaturized calorimetry - a new method for real-time biofilm activity analysis, J. Microbiol. Methods 74 (2008) 74–81, https://doi.org/10.1016/j.mimet.2008.04.004.

[10] C. Dreszer, J.S. Vrouwenvelder, A.H. Paulitsch-Fuchs, A. Zwijnenburg, J.C. Kruithof, H.C. Flemming, Hydraulic resistance of biofilms, J. Membr. Sci. 429 (2013) 436–447, https://doi.org/10.1016/j.memsci.2012.11.030.

[11] Y.W. Kim, S.E. Sardari, M.T. Meyer, A.A. Iliadis, H.C. Wu, W.E. Bentley, R. Ghodssi, An ALD aluminum oxide passivated Surface Acoustic Wave sensor for early biofilm detection, Sensor. Actuator. B Chem. 163 (2012) 136–145, https://doi.org/10.1016/j.snb.2012.01.021.

[12] H.J. Byrne, M. Baranska, G.J. Puppels, N. Stone, B. Wood, K.M. Gough, P. Lasch, P. Heraud, J. Sulé-Suso, G.D. Sockalingum, Spectropathology for the next generation: quo vadis? Analyst 140 (2015) 2066–2073, https://doi.org/10.1039/c4an02036g.

[13] T. Sojinrin, J. Conde, K. Liu, J. Curtin, H.J. Byrne, D. Cui, F. Tian, Plasmonic gold nanoparticles for detection of fungi and human cutaneous fungal infections, Anal. Bioanal. Chem. 409 (2017) 4647–4658, https://doi.org/10.1007/s00216-017-0414-7.

[14] J.C. Tsang, J.R. Kirtley, J.A. Bradley, Surface-enhanced Raman spectroscopy and surface plasmons, Phys. Rev. Lett. 43 (1979) 772–775, https://doi.org/10.1103/PhysRevLett.43.772.

[15] M. Moskovits, Surface-enhanced Raman spectroscopy: a brief retrospective, J. Raman Spectrosc. 36 (2005) 485–496, https://doi.org/10.1002/jrs.1362.

[16] D.S. Kopitsyn, M.V. Gorbachevskii, E.A. Botchkova, M.A. Bychenko, A.A. Novikov, Identification of bacteria by surface-enhanced Raman spectra after peroxide treatment, Appl. Biochem. Microbiol. 55 (2019) 78–82, https://doi.org/10.1134/S0003683819010095.

[17] Z. Zhou, S. Peng, M. Sui, S. Chen, L. Huang, H. Xu, T. Jiang, Multifunctional nanocomplex for surface-enhanced Raman scattering imaging and near-infrared photodynamic antimicrobial therapy of vancomycin-resistant bacteria, Colloids Surf. B Biointerfaces 161 (2018) 394–402, https://doi.org/10.1016/j.colsurfb.2017.11.005.

[18] Y. Chao, T. Zhang, Surface-enhanced Raman scattering (SERS) revealing chemical variation during biofilm formation: from initial attachment to mature biofilm, Anal. Bioanal. Chem. 404 (2012) 1465–1475, https://doi.org/10.1007/s00216-012-6225-y.

[19] P. Chen, L. Cui, K. Zhang, Surface-enhanced Raman spectroscopy monitoring the development of dual-species biofouling on membrane surfaces, J. Membr. Sci. 473 (2015) 36–44, https://doi.org/10.1016/j.memsci.2014.09.007.

[20] S. Keleştemur, Z. Çobandede, M. Çulha, Biofilm formation of clinically important microorganisms on 2D and 3D poly (methyl methacrylate) substrates: a surface-enhanced Raman scattering study, Colloids Surf. B Biointerfaces 188 (2020) 110765, https://doi.org/10.1016/j.colsurfb.2019.110765.

[21] A.V. Gannesen, E.L. Zdorovenko, E.A. Botchkova, J. Hardouin, S. Massier, D.S. Kopitsyn, M.V. Gorbachevskii, A.A. Kadykova, A.S. Shashkov, M.V. Zhurina, A.I. Netrusov, Y.A. Knirel, V.K. Plakunov, M.G.J. Feuilloley, Composition of the biofilm matrix of cutibacterium acnes acneic strain RT5, Front. Microbiol. 10 (2019), https://doi.org/10.3389/fmicb.2019.01284.

[22] S. Juneja, J. Bhattacharya, Coffee ring effect assisted improved S. aureus screening on a physically restrained gold nanoflower enriched SERS substrate, Colloids Surf. B Biointerfaces 182 (2019) 110349, https://doi.org/10.1016/j.colsurfb.2019.110349.

[23] J.S. Maeng, N. Kim, C.T. Kim, S.R. Han, Y.J. Lee, S.W. Lee, M.H. Lee, Y.J. Cho, Rapid detection of food pathogens using RNA aptamers-immobilized slide, J. Nanosci. Nanotechnol. 12 (2012) 5138–5142, https://doi.org/10.1166/jnn.2012.6369.

[24] C.L.A. Hamula, H. Zhang, L.L. Guan, X.F. Li, X.C. Le, Selection of aptamers against live bacterial cells, Anal. Chem. 80 (2008) 7812–7819, https://doi.org/10.1021/ac801272s.

[25] S. Wu, N. Duan, C. He, Q. Yu, S. Dai, Z. Wang, Surface-enhanced Raman spectroscopic–based aptasensor for Shigella sonnei using a dual-functional metal complex-ligated gold nanoparticles dimer, Colloids Surf. B Biointerfaces 190 (2020) 110940, https://doi.org/10.1016/j.colsurfb.2020.110940.

[27] O. Žukovskaja, S. Agafilushkina, V. Sivakov, K. Weber, D. Cialla-May, L. Osminkina, J. Popp, Rapid detection of the bacterial biomarker pyocyanin in artificial sputum using a SERS-active silicon nanowire matrix covered by bimetallic noble metal nanoparticles, Talanta 202 (2019) 171–177, https://doi.org/10.1016/j.talanta.2019.04.047.

[28] G. Bodelón, V. Montes-García, V. López-Puente, E.H. Hill, C. Hamon, M.N. Sanz-Ortiz, S. Rodal-Cedeira, C. Costas, S. Celiksoy, I. Pérez-Juste, L. Scarabelli, A. La Porta, J. Pérez-Juste, I. Pastoriza-Santos, L.M. Liz-Marzán, Detection and imaging of quorum sensing in Pseudomonas aeruginosa biofilm communities by surface-enhanced resonance Raman scattering, Nat. Mater. 15 (2016) 1203–1211, https://doi.org/10.1038/nmat4720.

[29] X.R. Bai, Y. Zeng, X.D. Zhou, X.H. Wang, A.G. Shen, J.M. Hu, Environmentally safe mercury(II) ions aided zero-background and ultrasensitive SERS detection of dipicolinic acid, Anal. Chem. 89 (2017) 10335–10342, https://doi.org/10.1021/acs.analchem.7b02172.

[30] N.G. Bastús, J. Comenge, V. Puntes, Kinetically controlled seeded growth synthesis of citrate-stabilized gold nanoparticles of up to 200 nm: size focusing versus ostwald ripening, Langmuir 27 (2011) 11098–11105, https://doi.org/10.1021/la201938u.

[31] M.V. Gorbachevskii, D.S. Kopitsyn, M.S. Kotelev, E.V. Ivanov, V.A. Vinokurov, A.A. Novikov, Amplification of surface-enhanced Raman scattering by the oxidation of capping agents on gold nanoparticles, RSC Adv. 8 (2018) 19051–19057, https://doi.org/10.1039/c8ra00417j.

[32] Natick MATLAB, Version 7.10.0 (R2010a), Massachusetts MathWorks Inc., 2010, 2010.

[33] C.A. Lieber, A. Mahadevan-Jansen, Automated method for subtraction of fluorescence from biological Raman spectra, Appl. Spectrosc. 57 (2003) 1363–1367, https://doi.org/10.1366/000370203322554518.

[34] Y. Zhang, T.P. Shareena Dasari, H. Deng, H. Yu, Antimicrobial activity of gold nanoparticles and ionic gold, J. Environ. Sci. Health Part C Environ. Carcinog. Ecotoxicol. Rev. 33 (2015) 286–327, https://doi.org/10.1080/10590501.2015.1055161.

[35] C.E. Hoffmann, O. Rahn, The bactericidal and bacteriostatic action of crystal violet, J. Bacteriol. 47 (1944) 177–186, https://doi.org/10.1128/jb.47.2.177-186.1944.

[36] K. Maliyar, A. Mufti, R.G. Sibbald, The use of antiseptic and antibacterial agents on wounds and the skin, Local Wound Care for Dermatologists,Updates in Clin. Dermatol. (2020) 35–52, https://doi.org/10.1007/978-3-030-28872-3_5.

[37] M.V. Cañamares, C. Chenal, R.L. Birke, J.R. Lombardi, DFT, SERS, and single-molecule SERS of crystal violet, J. Phys. Chem. C 112 (2008) 20295–20300, https://doi.org/10.1021/jp807807j.

[38] S.S. Phugare, D.C. Kalyani, A.V. Patil, J.P. Jadhav, Textile dye degradation by bacterial consortium and subsequent toxicological analysis of dye and dye metabolites using cytotoxicity, genotoxicity and oxidative stress studies, J. Hazard Mater. 186 (2011) 713–723, https://doi.org/10.1016/j.jhazmat.2010.11.049.

[39] B.E. Barragán, C. Costa, M. Carmen Márquez, Biodegradation of azo dyes by bacteria inoculated on solid media, Dyes Pigments 75 (2007) 73–81, https://doi.org/10.1016/j.dyepig.2006.05.014.

[40] J.P. Jadhav, D.C. Kalyani, A.A. Telke, S.S. Phugare, S.P. Govindwar, Evaluation of the efficacy of a bacterial consortium for the removal of color, reduction of heavy metals, and toxicity from textile dye effluent, Bioresour. Technol. 101 (2010) 165–173, https://doi.org/10.1016/j.biortech.2009.08.027.

[41] N. Leopold, S. Cîntă-Pînzaru, M. Baia, E. Antonescu, O. Cozar, W. Kiefer, J. Popp, Raman and surface-enhanced Raman study of thiamine at different pH values, Vib. Spectrosc. 39 (2005) 169–176, https://doi.org/10.1016/j.vibspec.2005.02.019.

[42] C. Lutwak-Mann, The decomposition of adenine compounds by bacteria, Biochem. J. 30 (1936) 1405–1412, https://doi.org/10.1042/bj0301405.